Quantitative Proteomics of Strong and Weak Biofilm Formers of *Enterococcus faecalis* Reveals Novel Regulators of Biofilm Formation*[S]

Tanujaa Suriyanarayanan‡, Lin Qingsong§, Lim Teck Kwang§, Lee Yew Mun§, Thuyen Truong‡, and Chaminda Jayampath Seneviratne‡,¶

Enterococcus faecalis **is a bacterial pathogen associated with both endodontic and systemic infections. The biofilm formation ability of *E. faecalis* plays a key role in its virulence and drug resistance attributes. The formation of *E. faecalis* biofilms on implanted medical devices often results in treatment failure. In the present study, we report protein markers associated with the biofilm formation ability of *E. faecalis* using iTRAQ-based quantitative proteomics approach. In order to elucidate the biofilm-associated protein markers, we investigated the proteome of strong and weak biofilm-forming *E. faecalis* clinical isolates in comparison with standard American Type Culture Collection (ATCC) control strains. Comparison of *E. faecalis* strong and weak biofilm-forming clinical isolates with ATCC control strains showed that proteins associated with shikimate kinase pathway and sulfate transport were up-regulated in the strong biofilm former, while proteins associated with secondary metabolites, cofactor biosynthesis, and tetrahydrofolate biosynthesis were down-regulated. In the weak biofilm former, proteins associated with nucleoside and nucleotide biosynthesis were up-regulated, whereas proteins associated with sulfate and sugar transport were down-regulated. Further pathway and gene ontology analyses revealed that the major differences in biofilm formation arise from differences in metabolic activity levels of the strong and weak biofilm formers, with higher levels of metabolic activity observed in the weak biofilm former. The differences in metabolic activity could therefore be a major determinant of the biofilm ability of *E. faecalis*. The new markers identified from this study can be further characterized in order to understand their exact role in *E. faecalis* biofilm formation ability. This, in turn, can lead to numerous therapeutic benefits in the treatment of this oral and systemic pathogen. The data has been deposited to the ProteomeXchange with identifier PXD006542.** ***Molecular & Cellular Proteomics 17: 10.1074/mcp.RA117.000461, 643–654, 2018.***

Enterococcus faecalis is a Gram-positive, facultative anaerobic coccus usually considered as a harmless commensal in the gastrointestinal tract of humans (1). However, recent surveillance data indicate that *E. faecalis* is emerging as a leading pathogen in nosocomial infections accounting for about 90% of all cases of life-threatening enterococcal infections such as bacterial endocarditis, urinary tract infections, wound infections, and bacteremia leading to complications like meningitis, among others (2–4). In addition, *E. faecalis* is also greatly associated with root canal (endodontic) infections in the field of dentistry (5–7).

The success of *E. faecalis* as a clinical pathogen lies in its virulence attributes, including biofilm formation. *E. faecalis* is able to adhere to surfaces and form surface-attached microbial communities embedded in a matrix of extracellular polymeric substances known as biofilms (8–11). The National Institutes of Health estimates that as many as 80% of bacterial infections involve biofilm mode of growth, which contributes significantly to morbidity and mortality (12).

E. faecalis biofilm infections are extremely difficult to treat, especially when biofilms are formed on implanted medical devices. Hence, biofilm formation of *E. faecalis* is directly associated with therapeutic failure. In the field of dentistry, *E. faecalis* is known to form biofilms in the root canals of teeth that cause treatment failure, adding heavy economic burden (6, 13–15).

Strategies to combat the biofilm formation of *E. faecalis* can lead to potential therapeutic benefits. However, there is currently a limited understanding of the factors associated with biofilm formation of *E. faecalis*. Though, some of the previous genetic screening studies have suggested the role of genes coding for enterococcal surface protein *Esp*, aggregation

From the ‡Oral Sciences, Faculty of Dentistry, National University of Singapore; §Department of Biological Sciences, Faculty of Science, National University of Singapore

Received November 14, 2017, and in revised form, December 21, 2017

Published, MCP Papers in Press, January 22, 2018, DOI 10.1074/mcp.RA117.000461

Author contributions: T.S., L.Q., and C.J.S. designed the research; T.S. and L.T.K. performed the research; T.S., L.Q., L.T.K., L.Y.M., and C.J.S. analyzed the data; and T.S., T.T., and C.J.S. wrote the paper.

substance AS, gelatinase GelE, and quorum sensing system Fsr in *E. faecalis* biofilm formation, the association has always not been clear due to conflicting literature reports (16–21). Moreover, previous proteomics studies on *E. faecalis* have been largely focused on the evaluation of the differential protein expression patterns in planktonic *E. faecalis* cells exposed to antibiotics or to stress conditions (22–26).

In the current study, we have addressed this knowledge gap by employing an iTRAQ-based proteomics analysis of *E. faecalis* biofilms. The present study took a novel approach to examine the protein expression profiles of *E. faecalis* biofilms by comparing the proteomics profile of strong and weak biofilm-forming clinical isolates with commonly used ATCC laboratory isolates. This new approach and the comprehensive examination of proteomics profiles helped in obtaining direct evidence on biofilm regulators and the possible mechanisms governing biofilm formation of *E. faecalis*.

EXPERIMENTAL PROCEDURES

Bacterial Strains and Growth Conditions—Strong and weak biofilm-forming *E. faecalis* clinical isolates, namely Ef 63 and Ef 64, derived from patients with failed root canal treatments, were included in the current study (7, 27). Standard laboratory strains *E. faecalis* ATCC 29212 and *E. faecalis* ATCC 51299 were used as the control strains. Bacterial strains were cultured overnight in Brain-Heart Infusion broth (Oxoid, Singapore) at 37°C under shaking conditions prior to each experiment.

Biofilm Formation—E. faecalis biofilms were formed as described previously (28). Briefly, overnight cultures of *E. faecalis* isolates were harvested, washed with PBS, and resuspended in the culture medium to $\sim 10^7$ cells/ml. The cells were then seeded into the wells of a flat-bottomed, polystyrene microtiter plate and incubated at 37 °C for 48 h to allow for biofilm formation. Biofilm formation for each of the four *E. faecalis* isolates included in the study was performed in biological replicates.

Protein Extraction from E. faecalis Biofilms—*E. faecalis* biofilm proteins were extracted by harvesting and pelleting the biofilm cells. The resultant pellets were washed once with PBS and then resuspended in a buffer containing 0.5 M triethylammonium bicarbonate, pH 8.5, and 1% SDS. The resuspended cells were homogenized in a Micro Smash MS-100 beater (Tomy Seiko Co., Ltd., Japan) with 0.5-mm glass beads in screw cap tubes at a pulse of 4,000 rpm for 20 s in 8eight cycles. The homogenized cells were centrifuged to obtain the proteins in the supernatant. Protein estimation was carried out using Bradford assay (Bio-Rad). 100 μg proteins from each sample were used for iTRAQ[1] labeling.

iTRAQ Labeling and Sample Cleanup—100 μg of proteins extracted from the *E. faecalis* isolates 63, 64, 51299, and 29212 were labeled using iTRAQ Reagent 8-plex kit (SCIEX) according to the manufacturer's instructions with slight modifications. The first set of biological replicates for *E. faecalis* isolates Ef 63, Ef 64, ATCC 51299, and ATCC 29212 was labeled with labeling reagents 113, 114, 115, and 116, respectively. The second set of biological replicates for *E. faecalis* isolates Ef 63, Ef 64, ATCC 51299, and ATCC 29212 was labeled with labeling reagents 117, 118, 119, and 121, respectively. The iTRAQ labeling workflow is represented in Fig. 1. Briefly, protein samples were reduced with 5 mM TCEP at 65 °C for 60 min, alkylated with 10 mM MMTS for 15 min at room temperature, and then digested with trypsin (Promega) in the ratio of 1:20 at 37 °C for 16 h. The digested protein samples were labeled with iTRAQ reagent labels according to the manufacturer's protocol at room temperature for 2 h. Following this, the eight iTRAQ-labeled peptide samples were combined into a single centrifuge tube and were subjected to strong cation exchange to remove interfering substances such as excess iTRAQ reagent labels, organic solvent, and SDS according to the manufacturer's protocol (SCIEX). The resultant elutes were desalted using Sep-Pak C18 cartridges (Water), and lyophilized before reconstitution in 20 mM ammonium formate in water of pH 10 for two-dimensional liquid chromatography (2D-LC) separation.

2D LC-MS/MS Analysis—2D LC-MS/MS analysis was carried out as described previously (29, 30). Briefly, the peptides were first separated with the 1290 Infinity LC system (Agilent) linked with a reversed-phase column to achieve the first dimension of the peptide separation. Approximately 100 μg of the labeled peptides mixture reconstituted in 20 mM ammonium formate in water, pH 10, were injected using the micro-pickup loop mode into an Xbridge C18 column (C18, 3.5 μm, 3.0 mm $\times$ 150 mm, Waters Corp., Milford, MA). Mobile phase A consisting of 20 mM ammonium formate in water, pH 10, and mobile phase B consisting of 20 mM ammonium formate in 80% acetonitrile, pH 10, were used. The flow rate was set at 0.2 ml/min, and a total of 96 elute fractions were collected on a 96-well v-bottom plate using step gradients of mobile B: 0% for 10 min, 0–80% for 60 min, held at 80% for 5 min, 80–100% for 1 min, held at 100% for 5 min, 100–0% for 1 min, held at 0% for 14 min. The eluted fractions were pooled into ten fractions and desalted with Sep-Pak® tC18 _Elution Plate (186002318, Waters Corp.) using a vacuum manifold (Millipore) before second dimension reversed-phase chromatography. The desalted pooled sample was then lyophilized and reconstituted with 98% water, 2% acetonitrile with 0.1% formic acid. Peptides were separated on the second dimension of peptide separation using nanoLC Ultra and ChiPLC-nanoflex (Eksigent, Dublin, CA) in Trap Elute configuration. The samples were loaded on a 200 μm $\times$ 0.5 mm column (ChromXP C18-CL, 3 μm) and eluted on an analytical 75 μm $\times$ 15 cm column (ChromXP C18-CL, 3 μm). Mobile phase A containing 2% acetonitrile in H_2O and 0.1% formic acid and mobile phase B containing 98% acetonitrile in H_2O and 0.1% formic acid were used. The flow rate was set at 0.3 μl/min with the following gradient elution for peptide separation: 5 to 5% of mobile phase B in 1 min, 5 to 12% of mobile phase B in 19 min, 12 to 30% of mobile phase B in 120 min, 30 to 70% of mobile phase B in 10 min, 70 to 90% of mobile phase B in 2 min, 90 to 90% in 7 min, 90 to 5% in 6 min, and held at 5% of mobile phase B for 10 min.

MS analysis was performed in information-dependent mode using a 5600 TripleTOF analyzer (QqTOF; AB SCIEX). Precursor ions were selected across a mass range of 400–1800 *m/z* using 250 ms accumulation time per spectrum. A maximum of 20 most abundant precursor ions per cycle from each MS spectra were selected for MS/MS analyses with 100 ms accumulation time for each precursor, with a dynamic exclusion of 15 s. MS/MS recording was carried out in high sensitivity mode with rolling collision energy and with the iTRAQ reagent collision energy adjustment turned on.

[1] The abbreviations used are: iTRAQ, isobaric tags for relative and absolute quantitation; LC-MS/MS, liquid chromatography-tandem mass spectrometry; TOF, time of flight; 2D-LC, two-dimensional liquid chromatography; ABC, ATP-binding cassette; ATCC, American Type Culture Collection; BINGO, Biological Network Gene Ontology tool; BLAST, Basic Local Alignment Search Tool; ID, identification; iTRAQ, isobaric tags for relative and absolute quantitation; LC-MS/MS, liquid chromatography-tandem mass spectrometry; MMTS, Methyl methane-thiosulfonate; NCBI, National Center for Biotechnology Information; ROK, repressor, open reading frame, kinase; TOF, time of flight; UDP, uridine diphosphate.

Peptide and Protein Identification—Peptide identification and quantification was carried out on the ProteinPilot 5.0 software Revision 1656 (AB SCIEX) using the Paragon™ algorithm and the integrated false discovery rate (FDR) analysis function. In addition, further processing was conducting using the Pro Group™ algorithm where isoform-specific quantification was employed to determine potential differences between the expressions of various isoforms. This Pro Group algorithm involves calculating the protein ratios using only ratios generated from the spectra that are unique to each protein or protein isoform. This would eliminate any masking of changes in expression that results from peptides that are shared between proteins. The data were searched against a protein sequence database downloaded from UniProtKB for *E. faecalis* 29212 on February 2, 2016. To increase the specificity of the search, these protein sequence data are added with the international protein index human protein sequence database from the last release (July 2012). The following user-defined search parameters were used for the obtained MS/MS spectra: sample type: iTRAQ 8-plex (peptide labeled); cysteine alkylation: methyl methane-thiosulfonate (MMTS); digestion: trypsin; instrument: TripleTOF5600; special factors: none; species: none; identification (ID) focus: biological modification; database: uniprot_efaecalis_ipi_human.fasta; search effort: thorough; FDR analysis: yes. For the iTRAQ quantification, the peptide used for quantification was automatically selected based on the Pro Group algorithm to determine the reporter peak area, error factor, and ρ-value. The resultant data were subjected to auto bias-correction to remove any possible variations arising from unequal mixing during the combination of different labeled samples. The ProteinPilot software calculates the median ratio of all identified proteins based on an internal reference channel In order to account for potential iTRAQ ratio compression, background correction was performed to make fold changes closer to their actual values as described by Strbenac *et al.*, and this function of the ProteinPilot software uses one of the best algorithms to serve this purpose (31). The ProteinPilot software counts each iTRAQ-modified peptide as unique to each identified protein. The peak areas and the signal-to-noise ratios were extracted from the database by ProteinPilot to translate the raw data into a quantifiable data for downstream analysis.

The FDR determination of the data was subsequently conducted by searching against the concatenated databases made up of *in silico* on-the-fly reversal for decoy sequences that were generated automatically by the software based on our combined *E. faecalis* UniProtKB and human ipi search database. The unused protein score of $\geq$1.3 was used as the cutoff for correctly identified proteins, corresponding to 0.4% FDR. The FDR was calculated using the number of false positive hits as indicated by the reversed sequences over the total number of proteins after applying the cutoff of $\geq$1.3 unused protein score. The results were then exported into Microsoft Excel for manual data interpretation. The cutoff threshold for up-regulation and down-regulation of proteins was determined using population statistics applied to the biological replicates as proposed by Gan *et al.* (32, 33).

After determining the cutoff threshold, the four iTRAQ ratios obtained from each of the biological replicates of Ef 63 or Ef 64 over the biological replicates of the control Ef 51299 or Ef 29212 (*e.g.* 113/115, 113/116, 117/115, and 117/116) were subjected to the one sample *t* test analysis to determine significant change in protein abundance. The iTRAQ ratios were transformed by $\log_2$ before averaging them. These sets of four iTRAQ ratios were compared with a set of four dummy ratios of zero that represents no changes in protein abundance. A one sample *t* test was then conducted to evaluate whether the iTRAQ ratio of a protein is truly different from the mean of zero. Only the proteins showing p values < 0.05 for their mean iTRAQ ratios were considered statistically significant and were selected for further analysis.

Gene Ontology Analysis—The identified proteins were subjected to gene ontology analysis using Cytoscape (v2.8.3) (34) with Biological Network Gene Ontology Tool (BINGO) plugin (v2.44) (35). The resultant network figures were exported and visualized for overrepresentation of pathways as described previously (36).

RNA Extraction and Real-time PCR—RNA was extracted from 48 h *E. faecalis* biofilms using Qiagen RNeasy Protect Bacteria Mini Kit, followed by reverse transcription and real-time PCR analysis to test for the gene expression levels as previously described (27). Primer sequences for the genes of interest were generated using National Center for Biotechnology Information (NCBI) primer-Basic Local Alignment Search Tool (BLAST) search. The list of primers used in this study is provided in Supplemental Table 1.

Experimental Design and Statistical Rationale—48 h grown *E. faecalis* biofilms were collected for iTRAQ-based mass spectrometry analysis. Biofilm proteins were extracted from two independent sets of each of the four strains Ef 63, Ef 64, Ef 51299, and Ef 29212 and were included as biological replicates in the iTRAQ study (Fig. 1). Protein expression profiles of the two control strains Ef 51299 and Ef 29212 were taken as the basis for determining the up-regulation/down-regulation patterns in the strains Ef 63 and Ef 64. Proteins meeting the required cutoff threshold ratios (Figs. 2 and 3) and showing significant differential expression (One sample *t* test p value $<$ 0.05) were considered as up-regulated or down-regulated based on their expression patterns. Only the proteins that are up-regulated/down-regulated wrt both Ef 51299 and 29212 were included for further gene ontology and pathway enrichment analysis. For real-time PCR analysis, RNA was extracted from four different biological replicates of the strains Ef 63, Ef 64, Ef 51299, and Ef 29212. Real-time PCR analysis was performed using four biological replicates and two technical replicates each. Significance of the results was analyzed following analysis of variance. Differences were considered significant when p values are less than 0.05.

RESULTS

iTRAQ-based Quantitative Analysis of the Proteome of E. faecalis Isolates Ef 63 and Ef 64—In order to identify the biomarkers associated with the biofilm formation ability of *E. faecalis*, an iTRAQ-based mass spectrometry quantitative analysis was performed. Previously, we found that *E. faecalis* clinical isolates Ef 63 and Ef 64 had significantly stronger and weaker biofilm formation ability, respectively, when compared with that of the two ATCC strains of *E. faecalis* (27). *E. faecalis* ATCC strains 51299 and 29212 showed comparable levels of biofilm formation, and both were included for iTRAQ analysis in order to increase the robustness of comparison with the strong and the weak biofilm forming *E. faecalis* isolates (Fig. 1). A qualification criterion of unused protein score $\geq$1.3 (was used to obtain a total of 1412 proteins from the analysis. The corresponding global FDR for the unused score of $\geq$1.3 was 0.4%. The differential expression analysis of the proteome was performed by comparing the strong and the weak biofilm-forming *E. faecalis* isolates Ef 63 and Ef 64 against each of the ATCC strains individually. Analysis of fold changes of Ef 63 *versus* ATCC 51299 (113:115, 113:119, 117:115, 117:119), Ef 63 *versus* ATCC 29212 (113:116, 113: 121, 117:116, 117: 121), Ef 64 *versus* ATCC 51299 (114:115, 114:119, 118:115, 118:119), and Ef 64 *versus* ATCC 29212 (114:116, 114:121,

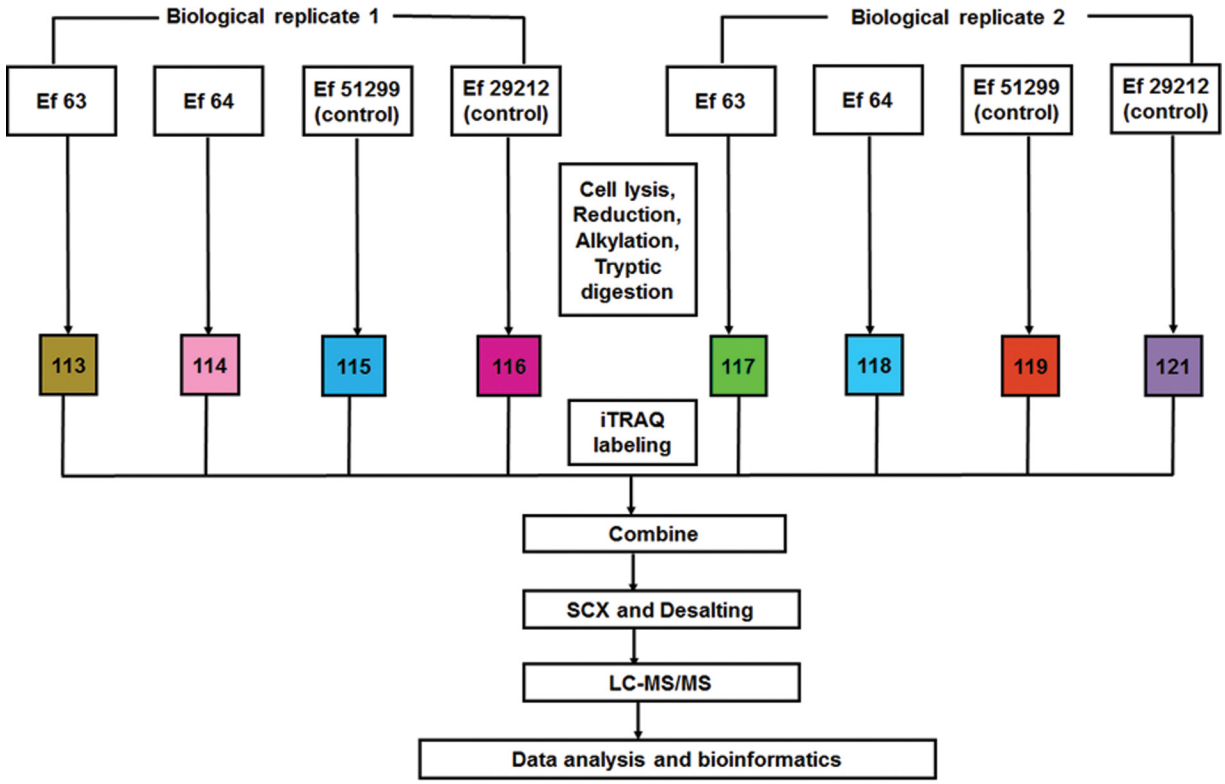

FIG. 1. **Experimental workflow for iTRAQ labeling and analysis:** iTRAQ 8-plex labeling was performed for two sets of biological replicates of the strains Ef 63, Ef 64, ATCC 51299, and ATCC 29212. Each strain was labeled as follows for the two biological replicates: Ef 63 (113, 117), Ef 64 (114, 118), ATCC 51299 (115, 119), and ATCC 29212 (116, 121). The labeled fractions were combined and subjected to strong cation exchange chromatography and desalting, followed by separation using liquid chromatography mass spectrometry (LC-MS/MS), and bioinformatics data analysis.

118:116, 118:121) was carried out to get the differential expression profiles. The obtained fold changes were then filtered using population statistics to get the significant threshold cutoff of up-regulated and down-regulated proteins for each of the comparisons performed in the study. Percentage variations corresponding to 88% coverage were taken as the threshold cutoff and any values outside 88% were considered as significantly altered. Based on these population statistics, the following cutoff fold change values were obtained for Ef 63 *versus* ATCC 51299 set: >1.5-fold and <0.67 (1/1.5)-fold for up-regulated and down-regulated proteins corresponding to 50% variation, Ef 64 *versus* ATCC 51299: >1.5-fold and <0.67 (1/1.5)-fold for up-regulated and down-regulated proteins corresponding to 50% variation, Ef 63 *versus* ATCC 29212: >1.5-fold and <0.67 (1/1.5)-fold for up-regulated and down-regulated proteins corresponding to 50% variation, and Ef 64 *versus* ATCC 29212: >1.75-fold and <0.57 (1/1.75)-fold for up-regulated and down-regulated proteins corresponding to 75% variation (Fig. 2).

The profile of differentially expressed proteins in each comparison were represented using volcano plots by applying the fold change and *p* value cutoff values (Fig. 3). The proteins with fold changes beyond the cutoff values obtained from Fig. 2 and with *p* values < 0.05 were considered as the most significantly affected proteins in each comparison.

Identification of Differentially Regulated Proteins in the Strong and Weak Biofilm-forming E. faecalis Isolates Ef 63 and Ef 64—In order to identify the proteins that could be associated with the biofilm formation ability of *E. faecalis*, the list of differentially regulated proteins obtained from the previous analysis were further scrutinized and combined for a more robust comparison. Following a comparison of the strong and the weak biofilm-forming strains with both the ATCC control strains, only the list of proteins that were showing significant up-regulation or down-regulation with respect to both 51299 and 29212 were selected as significantly up-regulated and down-regulated in the strong and the weak biofilm formers.

(a) Up-regulated Proteins in the Strong Biofilm Former Ef 63—The proteins that are significantly up-regulated in the strong biofilm former Ef63 in comparison with both the ATCC strains are listed in Table I. Of these proteins, shikimate kinase encoded by *aroK*, and 5-enolpyruvylshikimate-3-phosphate synthase encoded by *aroA* are enzymes involved in the intermediate and penultimate steps of the shikimate pathway, which is essential for the synthesis of aromatic amino acids in

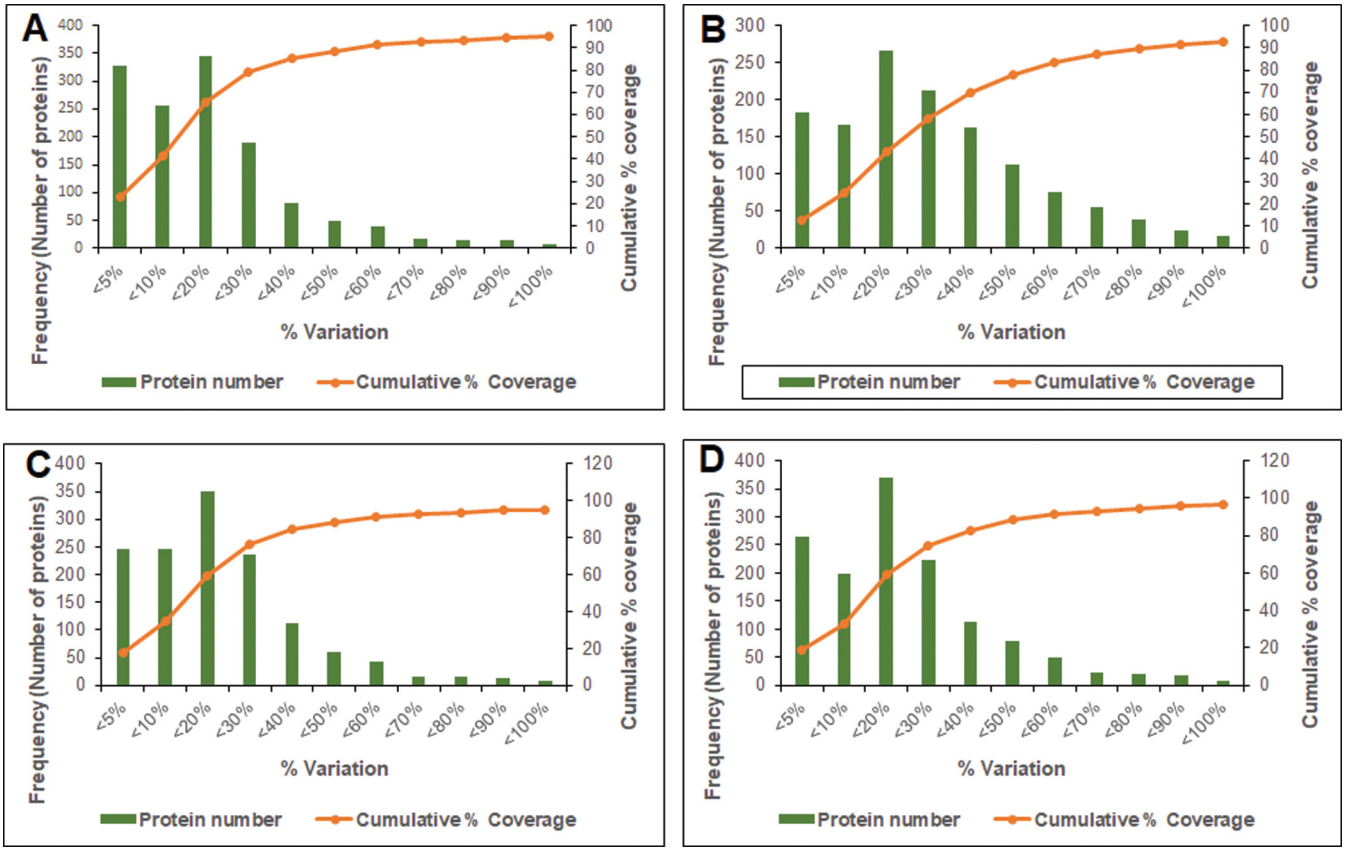

FIG. 2. **Determination of experimental variation for the identified proteins:** (*A*) experimental variation of Ef 63 compared with ATCC 29212; (*B*) experimental variation of Ef 64 compared with ATCC 29212; (*C*) experimental variation of Ef 63 compared with ATCC 51299; and (*D*) experimental variation of Ef 64 compared with ATCC 51299. The horizontal axis represents % variation of iTRAQ ratios. The primary vertical axis represents the corresponding number of proteins (bars) having different % variation. The secondary vertical axis represents the cumulative % of the counted proteins. Variation against 88% coverage of population was considered as the cutoff value.

bacteria (37, 38). Trehalose-6-phosphate encoded by *trePP* is a part of trehalose metabolic pathway (39). Other up-regulated proteins include prepentate dehydratase encoded by *pheA*, which is a part of the phenylalanine biosynthesis pathway and a sulfate permease protein encoded by *ychM*, belonging to sulfate transporter/secondary anion transporters superfamily (40, 41). Members of the phage family protein, a putative oxidoreductase DR75_1429, and hypothetical proteins DR75_2587, DR75_1646, and DR75_1626 were also up-regulated. Hypothetical protein DR75_2587 belongs to a putative lipoprotein family based on NCBI BLAST results.

(b) Up-regulated Proteins in the Weak Biofilm Former Ef 64—The proteins that are up-regulated in the weak biofilm former Ef 64 are listed in Table II. Of these, orotidine-5-phosphate decarboxylase encoded by *pyrF*, dihydroorotase encoded by *pyrA*, orotate-phosphoribosyltransferase encoded by *pyrE*, and carbamoyl synthase encoded by *carA* are enzymes belonging to *de novo* pyrimidine nucleobase and nucleotide biosynthetic process. Bifunctional protein encoded by *pyrR* is a transcriptional regulator of the pyrimidine nucleotide operon. Other up-regulated proteins include ribosome recycling factor encoded by *frr*, which helps in the dissociation of ribosomes from the mRNA upon completion of translation and is essential for cell growth, and hypothetical proteins DR75_2329 and DR75_910 (42).

(c) Down-regulated Proteins in the Strong Biofilm Former Ef 63—The proteins that are down-regulated in the strong biofilm former Ef 63 are listed in Table III. Of these, DNA protection during starvation protein encoded by *dps* confers DNA protection during stationary phase, and galactose mutarotase encoded by *galM* is part of galactose metabolism (43, 44). Aspartate-1-decarboxylase encoded by panD, dihydroneopterin aldolase encoded by *folB*, and serine O-acetyltransferase encoded by *cysE* are enzymes involved in metabolic pathways such as biosynthesis of secondary metabolites, cofactor biosynthesis, and tetrahydrofolate biosynthesis. DR75_2966 and DR75_2967 are replication-associated proteins belonging to plasmids or mobile genetic elements of Gram-positive bacteria (45, 46). DR75_634 represents an ethanolamine two-component response regulator, which belongs to a phosphor-relay system. DR75_1696 and DR75_1697 are proteins belonging to the phosphoenol-pyruvate-dependent sugar transport system (PTS) responsible for the transport of ascorbate and lactose respectively.

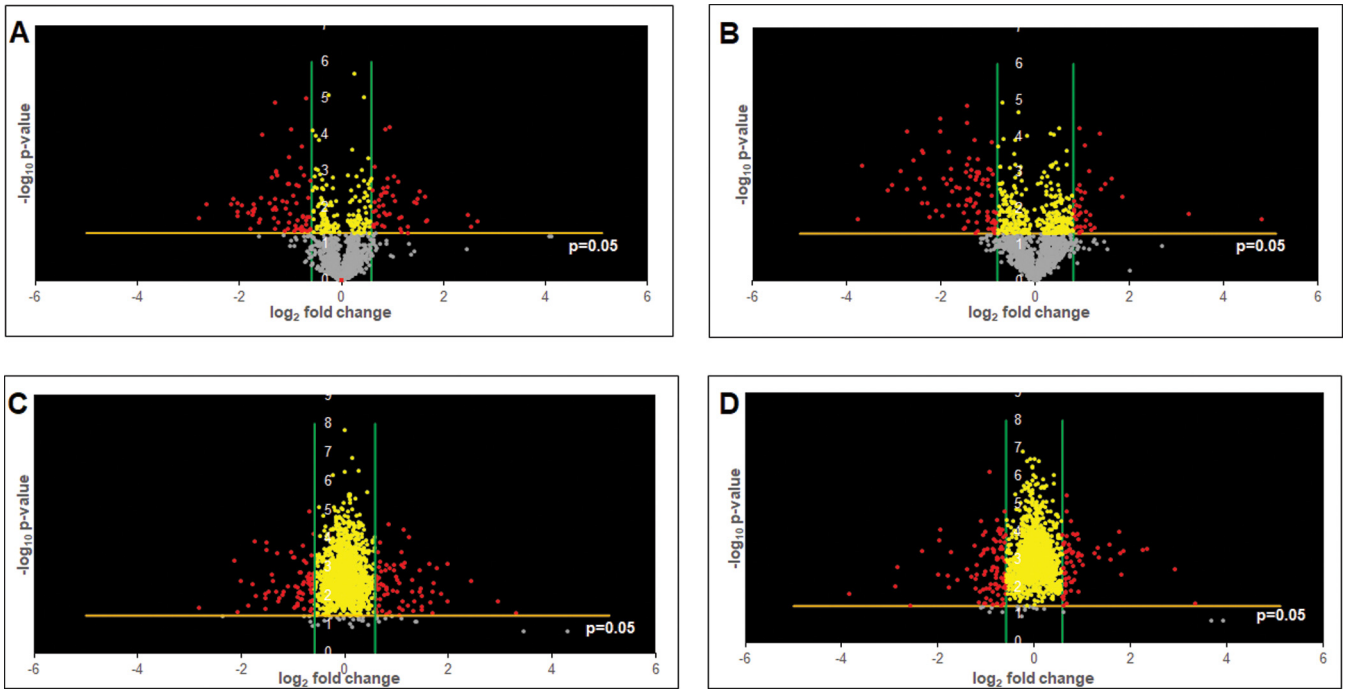

FIG. 3. **Volcano plots of differentially regulated proteins reveal significance patterns:** (*A*) volcano plots of differentially regulated proteins of Ef 63 compared with ATCC 29212; (*B*) volcano plots of differentially regulated proteins of Ef 64 compared with ATCC 29212; (*C*) volcano plots of differentially regulated proteins of Ef 63 compared with ATCC 51299; and (*D*) volcano plots of differentially regulated proteins of Ef 64 compared with ATCC 51299. Threshold cutoffs determined for $\log_2$ fold change ratios are represented by green lines. *p* value cutoff of 0.05 is represented by a yellow line. Gray dots represent proteins that do not show significant differences in expression, yellow dots represent proteins that show significant differences in expression but within the cutoff $\log_2$ fold change ratios, and red dots represent proteins that show significant differences in expression outside the cut-off $\log_2$ fold change ratios.

TABLE I

Functional classification of the significantly up-regulated proteins of Ef 63 in comparison with both ATCC 29212 and 51299 strains meeting both *p* value cutoff and $\log_2$ fold-change cutoff criteria

Proteins upregulated in 63						
Accession #	Protein name	Gene name	Unused protein score	Peptides (95%)	Fold change wrt 29212	Fold change wrt 51299
UPI00032E9DD8	3-phosphoshikimate 1-carboxyvinyl transferase; 5-enolpyruvylshikimate-3-phosphate synthase	aroA; DR75_569	26.4	26	3.110713011	3.409029024
UPI000291C4DE	Trehalose 6-phosphate phosphorylase	trePP	18.68	13	3.023335133	1.983570371
UPI00019F352C	Shikimate kinase (SK) (EC 2.7.1.71); shikimate kinase family protein	aroK; DR75_570	10.04	5	2.480368467	3.124256418
UPI000005C662	Putative oxidoreductase YcjS; oxidoreductase, NAD-binding Rossmann fold family protein	DR75_1429	10	5	1.923075843	2.021658161
UPI0001E1A33D	Prephenate dehydratase	pheA; DR75_571	8	5	2.891981312	3.264071801
UPI0002910B7F	Phage major tail, phi13 family protein	DR75_1505	3.8	2	3.200903531	2.780474197
UPI00019F3544	Hypothetical protein	DR75_2587	2.18	2	2.823765229	1.523319053
UPI000291BF2D	Hypothetical protein	DR75_1646	2	2	2.783602486	2.472863241
UPI0001B1D951	Sulfate permease; sulfate permease family protein	ychm; DR75_1732	2	2	1.752083299	1.823848359
UPI0001B2BBD4	Hypothetical protein DR75_1626	DR75_1626	2	1	17.41533347	9.888407625

(d) Down-regulated Proteins in the Weak Biofilm Former Ef 64—The proteins that are down-regulated in the weak biofilm former Ef 64 are listed in Table IV. Of these, UDP-N-acetylenolpyruvoylglucosamine reductase encoded by *murB* is involved in peptidoglycan biosynthesis pathway, guanosine monophosphate reductase encoded by *guaC* is involved in purine ribonucleotide interconversion, and aspartate semialdehyde dehydrogenase encoded by *asd* is involved in amino acid biosynthesis. DR75_2512 represents a PTS sugar transport system responsible for sorbose transport and DR75_2078 represents an ROK family protein responsible for repressing xylose utilization. Sulfate permease and trehalose-6 phosphate phosphorylase proteins encoded by *ychM* and *trePP* are down-regulated in the weak biofilm former Ef 64 in contrast to their up-regulation in the strong biofilm former Ef 63. Aspartate 1-decarboxylase encoded by *panD* is down-regulated in both Ef 64 and Ef 63. Other down-regulated proteins include a putative lipoprotein

TABLE II

Functional classification of the significantly up-regulated proteins of Ef 64 in comparison with both ATCC 29212 and 51299 strains meeting both *p* value cutoff and $\log_2$ fold-change cutoff criteria

Proteins upregulated in 64						
Accession #	Protein names	Gene names	Unused protein score	Peptides (95%)	Fold change wrt 29212	Fold change wrt 51299
UPI000005C524	Ribosome-recycling factor (RRF) (ribosome-releasing factor)	frr;DR75_1144	36.78	64	1.906634	1.764784
UPI00019F32AD	Orotidine 5′-phosphate decarboxylase (EC 4.1.1.23) (OMP decarboxylase)	pyrF; DR75_712	20.48	12	2.080761	1.604881
UPI000005C2BD	Bifunctional protein PyrR	pyrR; DR75_720	18.04	14	2.086637	1.805877
UPI0001A5BFBD	Carbamoyl-phosphate synthase, small subunit	carA; DR75_716	18	11	1.980158	1.743035
UPI000175BF0F	Dihydroorotase(DHOase) (EC3.5.2.3)	pyrC; DR75_717	10	5	2.627464	2.391439
UPI000005C2B4	Orotate phosphoribosyl transferase (OPRT) (OPRTase) (EC 2.4.2.10)	pyrE; DR75_711	2.66	2	2.216797	1.530228
UPI0001B6DEC1	Hypothetical protein DR75_2329	DR75_2329	2.04	1	1.812651	7.603089

TABLE III

Functional classification of the significantly down-regulated proteins of Ef 63 in comparison with both ATCC 29212 and 51299 strains meeting both *p* value cutoff and $\log_2$ fold-change cutoff criteria

Proteins downregulated in 63						
Accession #	Protein names	Gene names	Unused protein score	Peptides (95%)	Fold change wrt 29212	Fold change wrt 51299
UPI000005C830	Dps family protein; DNA protection during starvation protein	dps; DR75_1942	25.85	74	0.158975959	0.141553384
UPI0001B1DD9C	Galactose mutarotase -aldose epimerase conserved domain	galM	19.17	13	0.649019509	0.549455743
UPI0000059961	Replication-associated protein RepB; cobQ/CobB/MinD/ParA nucleotide binding domain protein (plasmid)	DR75_2966	10.19	7	0.505973488	0.505026395
UPI00019C6B36	PTS system ascorbate-specific IIB component; PTS system, lactose/cellobiose specific IIB subunit	DR75_1696	8	8	0.242902381	0.518277773
UPI000005C334	Aspartate 1-decarboxylase (EC4.1.1.11) (aspartate alpha-decarboxylase)	panD; DR75_827	6.65	9	0.405554528	0.274218075
UPI000005C853	7,8-dihydroneopterin aldolase (EC4.1.2.25); dihydroneopterin aldolase	folB; DR75_1970	2.47	2	0.631259615	0.438989396
UPI0000059960	Replication-associated protein B; putative replication-associated protein (plasmid)	DR75_2967	2.08	1	0.388184377	0.292597088
UPI000005C269	Ethanolamine two-component response regulator; ANTAR domain protein	DR75_634	2	1	0.546653837	0.60537555
UPI0001B2588A	Glycerophosphoryl diester phosphodiesterase family protein	DR75_1000	2	1	0.57470862	0.297523575
UPI000005BCA4	Serine O-acetyltransferase	cysE; DR75_2093	2	1	0.399293872	0.34637114

TABLE IV

Functional classification of the significantly down-regulated proteins of Ef 64 in comparison with both ATCC 29212 and 51299 strains meeting both *p* value cutoff and log2-fold change cutoff criteria

Proteins downregulated in 64						
Accession #	Protein name	Gene name	Unused protein score	Peptides (95%)	Fold change wrt 29212	Fold change wrt 51299
UPI000005C57D	UDP-N-acetylenolpyruvoylglucosamine reductase	murB; DR75_1237	26.08	16	0.49488141	0.525412
UPI000291C4DE	Trehalose 6-phosphate phosphorylase	trePP	18.68	13	0.50414138	0.688992
UPI000175BDE7	Guanosine monophosphate reductase	guaC; DR75_1175	12.15	7	0.43528692	0.420406
UPI00019C74B7	PTS system IIB component; PTS system sorbose subIIB component family protein	DR75_2512	8.88	7	0.42363621	0.450195
UPI000005C334	Aspartate 1-decarboxylase (EC4.1.1.11) (aspartate alpha-decarboxylase)	panD; DR75_827	6.65	9	0.20464538	0.135274
UPI000005C0BA	Aspartate-semialdehyde dehydrogenase	asd	6	4	1.70472867	
UPI0001E19F8C	Hypothetical protein DR75_1765-possible peptidase	DR75_1765	5.77	3	0.3620089	0.300302
UPI000005BE6D	Xylose repressor; ROK family protein	DR75_2508	4.04	2	0.41415556	0.526703
UPI000005BC96	TdcF protein; reactive intermediate/imine deaminase family protein	DR75_2078	4.03	2	0.41691202	0.480218
UPI000290D069	Phage regulatory, Rha family protein	DR75_1539	4	3	0.83902121	0.87443
UPI0001B1D951	Sulfate permease	ychm; DR75_1732	2	2	0.522333	0.553958
UPI0001E1A077	Lipoprotein, putative	DR75_1236	2	1	0.3670319	0.382167
UPI000005C88A	Hypothetical protein	DR75_2043	2	1	0.15033957	0.139521

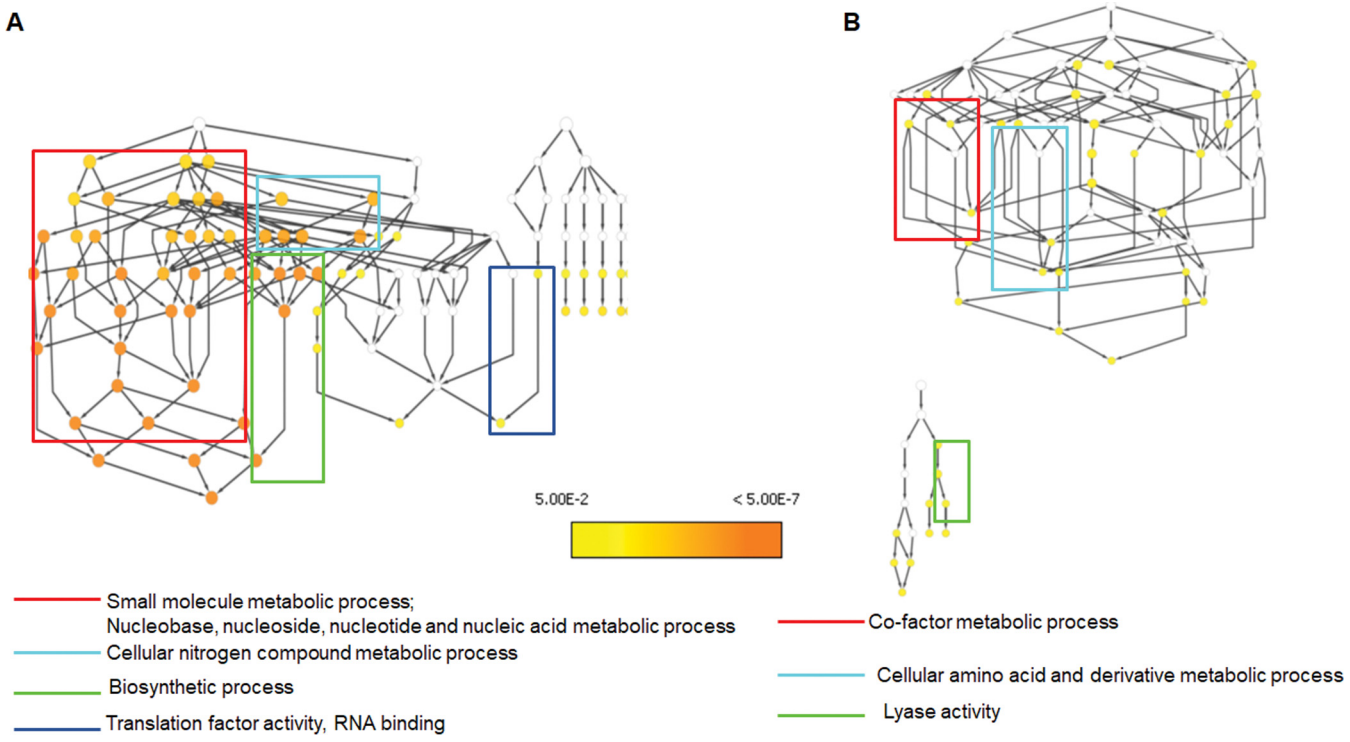

FIG. 4. **Gene ontology analysis of differentially regulated proteins reveals significantly affected pathways in Ef 63 and Ef 64:** (*A*) biological processes, molecular functions, and cellular components that are significantly up-regulated in Ef 64 in comparison with ATCC 29212 and 51299 strains and (*B*) biological processes, molecular functions, and cellular components that are significantly down-regulated in Ef 63 in comparison with ATCC 29212 and 51299 strains.

(DR75_1236), hydrolase (DR75_684), hypothetical proteins DR75_2043, and DR75_1811, which is a probable ABC transporter permease belonging to yitT family based on NCBI BLAST results.

Pathway Enrichment Analysis of the Up-regulated and the Down-regulated Proteins of Ef 63 and Ef 64—In order to test for pathway overrepresentation/enrichment, gene ontology analysis for the up-regulated and down-regulated proteins of the strong and weak biofilm formers was performed using BINGO Cytoscape plugin. The pathway enrichment analysis for each comparison was done under conditions GO_full and GO_slim categories. The GO_full analysis represents the full annotation of all the genes involved in various biological processes and molecular functions, whereas the GO_slim analysis represented only the generic pathways affected in each comparison set, corresponding to the bigger picture of pathways affected. The pathway enrichment analysis of up-regulated proteins in Ef 63 and down-regulated proteins in Ef 64 with respect to the two ATCC control strains did not result in any pathway mapping in the GO_slim analysis, whereas a network of biological processes and molecular functions, which were significantly affected was obtained in the GO_full analysis (Figs. S1 and S4). The analysis of the up-regulated proteins in Ef 64 with respect to the two control strains in GO_slim mode showed the pathways relating to small molecule metabolic process and nucleobase, nucleoside, nucleotide and nucleic acid metabolic process, cellular nitrogen compound metabolic process, biosynthetic process, and RNA-binding activity to be significantly up-regulated (Fig 4*A*). The full list of up-regulated biological processes and molecular functions is provided in Fig. S2. The analysis of the down-regulated proteins in Ef 63 with respect to the two control strains in GO_slim mode showed the pathways relating to cofactor metabolic process, cellular amino acid and metabolic derivative process, and lyase activity to be significantly down-regulated (Fig 4*B*). The full list of down-regulated biological processes and molecular functions is provided in Fig. S3. Based on this analysis, there are a higher number of metabolic processes up-regulated in Ef 64 and down-regulated in Ef 63, indicating higher metabolic activity in the weak biofilm former.

Correlation of iTRAQ Data with Quantitative Real-time PCR (qPCR) Results—In order to verify the reliability of the iTRAQ analysis, gene expression profiles of selected genes were obtained using qPCR. Representative genes for qPCR analysis were selected based on the most important pathways affected in each comparison and some of the unique transporter class proteins that are not represented in the pathway enrichment list. The significantly up-regulated and down-regulated gene expression profiles were obtained from qPCR (Fig 5*A*). The results obtained from qPCR analysis were then checked for their correlation with iTRAQ data by Pearson's

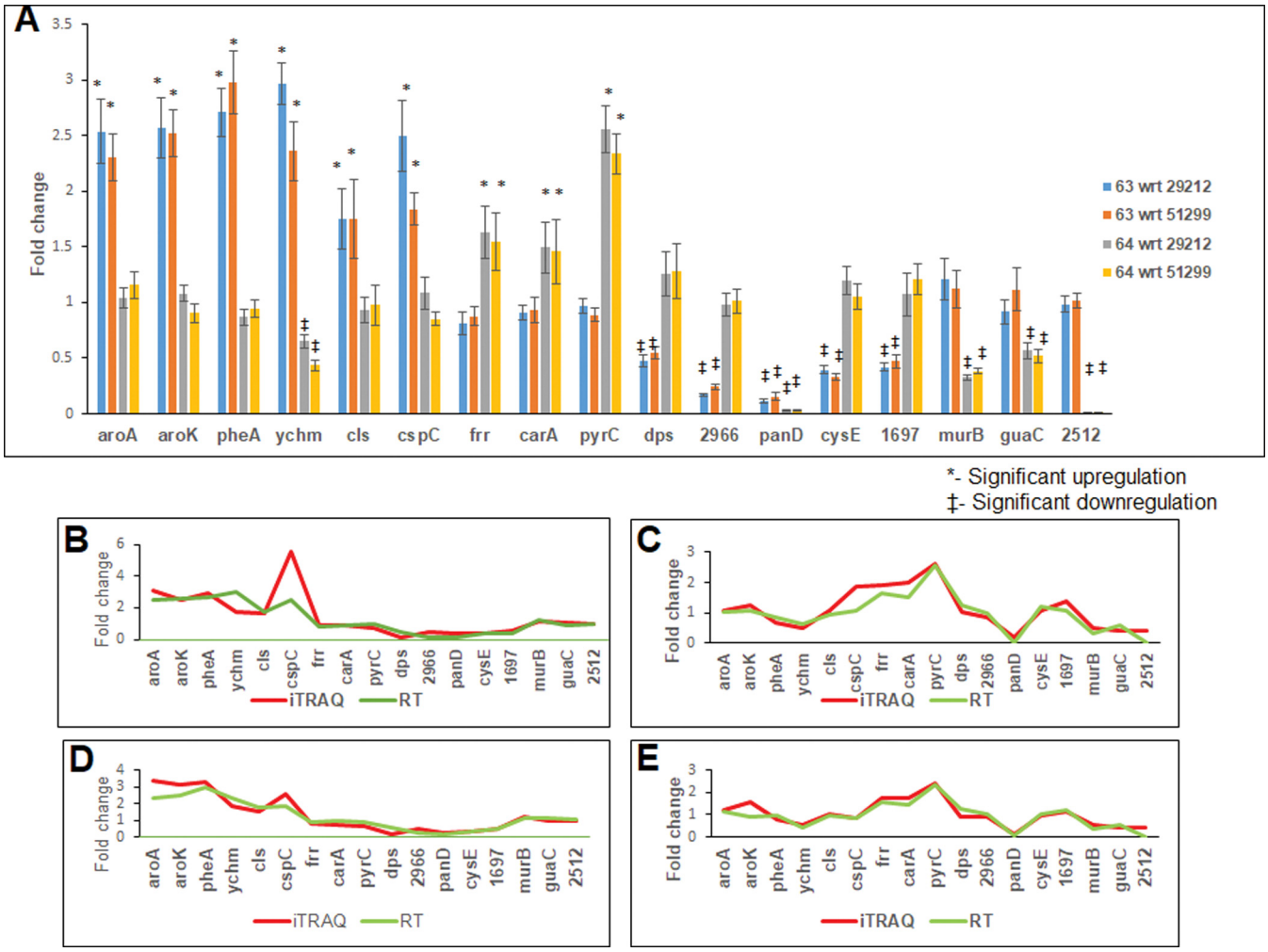

FIG. 5. **Quantitative real-time PCR analysis and correlation with iTRAQ data:** (*A*) quantitative real-time PCR analysis of selected significantly regulated genes obtained from iTRAQ analysis; (*B*) correlation of real-time gene expression data from *A* to iTRAQ protein expression data of 63 wrt 29212; (*C*) correlation of real-time gene expression data from *A* to iTRAQ protein expression data of 64 wrt 29212; (*D*) correlation of real-time gene expression data from *A* to iTRAQ protein expression data of 63 wrt 51299; and (*E*) correlation of real-time gene expression data from *A* to iTRAQ protein expression data of 64 wrt 51299.

correlation analysis. A significant positive correlation was obtained between the iTRAQ data and the qPCR results, which indicates that the gene expression profile and the protein expression profile follow a similar trend ensuring the reliability of iTRAQ analysis (Figs. 5*B*–5*E*).

DISCUSSION

Bacterial-biofilm-associated clinical problems have been described in a wide spectrum of Gram-positive as well as Gram-negative organisms, including *Staphylococcus aureus*, *Streptococcus mutans*, *E. faecalis*, *Pseudomonas aeruginosa*, and *Escherichia coli* (47, 48). However, the molecular markers and mechanism involved in *E. faecalis* biofilm formation is still not clearly understood. Previously, we found significant changes in the transcriptomic expression profile of *E. faecalis* isolates pertaining to several cellular and metabolic processes and transporters of the *E. faecalis* biofilm *versus* planktonic modes (27). Taking a step ahead, in this iTRAQ-based proteomics study, we specifically focused on the protein expression profiles of the strong and weak biofilm formers of *E. faecalis* in comparison to the ATCC laboratory strains.

Analysis of the protein profiles signatures across different strains elucidated interesting observations on metabolic processes, biosynthetic processes, and transport systems such as sugar transporters and sulfate permease involved in *E. faecalis* biofilm formation. For instance, the up-regulation of shikimate pathway proteins encoded by *aroA* and *aroK* in the strong biofilm former indicates an increased synthesis of aromatic amino acids in the strong biofilm former Ef 63. Certain studies have shown that the production of 5-enolpyruvylshikimate-3-phosphate synthase by *aroA* can lead to glyphosphate resistance in pathogenic bacteria such as *S. aureus* and the virulence, growth, and UV tolerance of the plant pathogen *Burkholderia glumae* (38, 49). This suggests that the strong

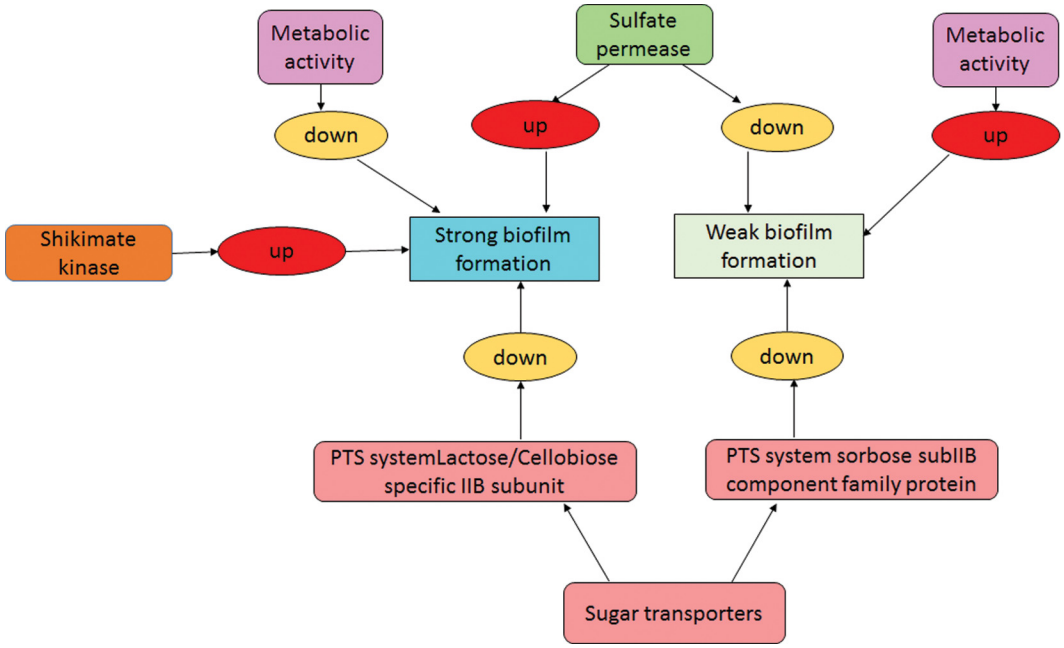

FIG. 6. Novel regulators of *E. faecalis* biofilm formation identified from iTRAQ analysis.

biofilm former Ef 63 can display increased levels of glyphosphate resistance and pathogenesis mechanisms, possibly resulting in higher biofilm formation. Similarly, up-regulation of sulfate permease encoded by *ychM* in the strong biofilm former Ef 63, and down-regulation of sulfate permease in the weak biofilm former Ef 64, suggests that sulfur uptake/secondary anions transport have a role in *E. faecalis* biofilm formation ability. Sulfur uptake has been shown to be important for the virulence of certain pathogenic bacteria such as *Mycobacterium tuberculosis* (41). In addition, links between sulfur uptake, c-di-GMP signaling and biofilm formation have been found in *Shewanella oneidensis,* where biofilm formation is reduced due to decrease in sulfur uptake (48). Therefore, the increased and decreased levels of sulfate permease found in the biofilms of Ef 63 and Ef 64 could be associated with the strong biofilm formation capability of Ef 63, and the weak biofilm formation capability of Ef 64, respectively, indicating the possible role of *ychM* as a regulator of biofilm formation in *E. faecalis*.

Sugar transporter systems such as PTS system, lactose/cellobiose-specific IIB subunit and PTS system sorbose subIIB component family protein are down-regulated in Ef 63 and Ef 64, respectively. This suggests that the active transport of lactose and sorbose are down-regulated in the strong and the weak biofilm formers, respectively. Though the exact correlation between the expression of sugar transporters and biofilm formation is still not clear, previous studies of *E. faecalis* proteome in response to bile stress have shown up-regulation of the IIAB component of a mannose-specific PTS system (26). Similarly, comparative proteomics of *E. faecalis* clinical isolates and food isolates showed IIA, IIBC, and IIATP-binding cassette (ABC) components of the PTS system to be up-regulated in the food isolates of *E. faecalis* (25). Taken together, this indicates that sugar transport systems are differentially regulated according to the stress response and the isolate nature and may be possibly linked to the biofilm formation ability of *E. faecalis*, depending on the nature of the sugar transport system affected.

The pathway enrichment analysis of the differentially regulated proteins using Cytoscape revealed interesting insights into the metabolic profiles of the strong and the weak biofilm formers Ef 63 and Ef 64. In the isolate Ef 64, small molecule, nucleotide, and nitrogen compound metabolic processes and biosynthetic pathways are significantly up-regulated, indicating a higher metabolic activity profile of the weak biofilm former. In the isolate Ef 63, cofactor metabolic process, cellular amino acid and derivative metabolic process, and lyase activity are significantly down-regulated, indicating a lower metabolic activity profile of the strong biofilm former. Previous studies comparing biofilm and planktonic states of *Streptococcus pneumoniae* have suggested that biofilm cells exhibit low metabolic activity (50–52). In addition, certain studies on *Burkholderia cenocepacia* and *P. aeruginosa* have shown that persister cells, which represent a subpopulation of biofilm cells, show a lowered metabolic activity state capable of conferring protection against antibiotics and harmful environmental conditions (10, 53–55). It is possible that the metabolically active biofilm cells promote dispersal instead of adhesion, resulting in biofilms with less mass. Hence, the differences in the metabolism may have contributed to the strong and weak biofilm-forming ability of Ef 63 and Ef 64, respectively. Metabolic regulation is also observed in some multispecies oral biofilm models. In a mixed-species biofilm model of *S. mutans*, differences in fatty acid biosynthesis and

branched chain amino acids metabolism were observed in the mixed-species biofilms in comparison with single-species biofilms (56). Similarly, in a mixed-species biofilm study of *Anaeroglobulus geminatus*, differentially regulated proteins were found to be involved in carbon metabolism, iron transport, and proteolysis. These studies show that constant changes in metabolic responses occur in bacterial biofilm systems in order to cope with a dynamically changing environment (57).

Correlation of the obtained iTRAQ data with RT-PCR results confirms the reliability of the analysis, serving as a validation for the novel regulators of biofilm formation identified from this study. In conclusion, this pioneering proteomics study has shed novel insights into the biofilm-forming ability of *E. faecalis*. It was found that the shikimate pathway, sugar and sulfate permease transporter systems, and metabolic profiles of *E. faecalis* may have a significant role in the biofilm formation of *E. faecalis* and its pathogenic traits (Fig. 6). Further studies using genetic knock-out mutants are warranted to elucidate the roles of the identified biomarkers associated with *E. faecalis* biofilm, which may possibly provide a new tool set to design novel treatment strategies for this recalcitrant bacterial pathogen.

DATA AVAILABILITY

The mass spectrometry proteomics data have been deposited to the ProteomeXchange Consortium via the PRIDE [1] partner repository with the dataset identifier PXD006542.

* This study was supported by NUS-Start-up (R-221-000-064-133) and NMRC (R-221-000-086-511) to C.J.S.

¶ To whom correspondence should be addressed: Oral Sciences, Faculty of Dentistry, National University of Singapore, Tel: (+65)-6779-5555, Fax: (+65)-6778-5742. Email: jaya@nus.edu.sg.

S This article contains supplemental material.

REFERENCES

1. Fisher, K., and Phillips, C. (2009) The ecology, epidemiology and virulence of Enterococcus. *Microbiology.* **155,** 1749–1757
2. Hidron, A. I., Edwards, J. R., Patel, J. R., Horan, T. C., Sievert, D. M., Pollock, D. A., and Fridkin, S. K. (2008) NHSN annual update: Antimicrobial-resistant pathogens associated with healthcare-associated infections: Annual summary of data reported to the National Healthcare Safety Network at the Centers for Disease Control and Prevention, 2006–2007. *Infect. Control Hosp. Epidemiol.* **29,** 996–1011
3. Hollenbeck, B. L., and Rice, L. B. (2012) Intrinsic and acquired resistance mechanisms in enterococcus. *Virulence* **3,** 421–433
4. Anders, D., and Bruun, N. E. (2013) *Enterococcus faecalis* infective endocarditis: Focus on clinical aspects. *Expert Rev. Cardiovasc. Ther.* **11,** 1247–1257
5. Stuart, C. H., Schwartz, S. A., Beeson, T. J., and Owatz, C. B. (2006) *Enterococcus faecalis*: Its role in root canal treatment failure and current concepts in retreatment. *J. Endod.* **32,** 93–98
6. Ricucci, D., and Siqueira, J. F., Jr. (2010) Biofilms and apical periodontitis: Study of prevalence and association with clinical and histopathologic findings. *J. Endod.* **36,** 1277–1288
7. Zhu, X., Wang, Q., Zhang, C., Cheung, G. S., and Shen, Y. (2010) Prevalence, phenotype, and genotype of *Enterococcus faecalis* isolated from saliva and root canals in patients with persistent apical periodontitis. *J. Endod*. **36,** 1950–1955
8. Mohamed, J. A., and Huang, D. B. (2007) Biofilm formation by enterococci. *J. Med. Microbiol.* **56,** 1581–1588
9. Garsin, D. A., Willems, R. J. (2010) Insights into the biofilm lifestyle of enterococci. *Virulence* **1,** 219–221
10. Donlan, R. M., and Costerton, J. W. (2002) Biofilms: Survival mechanisms of clinically relevant microorganisms. *Clin. Microbiol. Rev.* **15,** 167–193
11. Høiby, N., Bjarnsholt, T., Givskov, M., Molin, S., and Ciofu, O. (2010) Antibiotic resistance of bacterial biofilms. *Int. J. Antimicrob. Agents* **35,** 322–332
12. Cook, L. C., and Dunny, G. M. (2013) Effects of biofilm growth on plasmid copy number and expression of antibiotic resistance genes in *Enterococcus faecalis*. *Antimicrob. Agents Chemother.* **57,** 1850–1856
13. Chávez de Paz, L. (2007) Redefining the persistent infection in root canals: Possible role of biofilm communities. *J. Endod.* **33,** 652–662
14. Preethee, T., Kandaswamy, D., and Hannah, R. (2012) Molecular identification of an *Enterococcus faecalis* endocarditis antigen *efaA* in root canals of therapy-resistant endodontic infections. *J. Conserv. Dent.* **15,** 319–322
15. Al-Ahmad, A., Ameen, H., Pelz, K., Karygianni, L., Wittmer, A., Anderson, A. C., Spitzmüller, B., and Hellwig, E. (2014) Antibiotic resistance and capacity for biofilm formation of different bacteria isolated from endodontic infections associated with root-filled teeth. *J. Endod.* **40,** 223–230
16. Paganelli, F. L., Willems, R. J., and Leavis, H. L. (2012) Optimizing future treatment of enterococcal infections: Attacking the biofilm? *Trends Microbiol.* **20,** 40–49
17. Shankar, N., Lockatell, C. V., Baghdayan, A. S., Drachenberg, C., Gilmore, M. S., and Johnson, D. E. (2001) Role of *Enterococcus faecalis* surface protein *Esp* in the pathogenesis of ascending urinary tract infection. *Infect. Immun*. **69,** 4366–4372,
18. Tendolkar, P. M., Baghdayan, A. S., Gilmore, M. S., and Shankar, N. (2004) Enterococcal surface protein, *Esp,* enhances biofilm formation by *Enterococcus faecalis. Infect. Immun.* **72,** 6032–6039
19. Toledo-Arana, A., Valle, J., Solano, C., Arrizubieta, M. J., Cucarella, C., Lamata, M., Amorena, B., Leiva, J., Penadés, J. R., and Lasa, I. (2001) The enterococcal surface protein, *Esp*, is involved in *Enterococcus faecalis* biofilm formation. *Appl. Environ. Microbiol*. **67,** 4538–4545
20. Duggan, J. M., and Sedgley, C. M. (2007) Biofilm formation of oral and endodontic *Enterococcus faecalis*. *J. Endod.* **33,** 815–818
21. Sandoe, J. A., Witherden, I. R., Cove, J. H., Heritage, J., and Wilcox, M. H. (2003) Correlation between enterococcal biofilm formation in vitro and medical-device-related infection potential in vivo. *J. Med. Microbiol.* **52,** 547–550
22. Arntzen MØ Karlsk, I. L., Skaugen, M., Eijsink, V. G., and Mathiesen, G. (2015) Proteomic investigation of the response of *Enterococcus faecalis* V583 when cultivated in urine. *PLoS One* **10,** 1–17
23. Giard, J. C., Laplace, J. M., Rincé, A., Pichereau, V., Benachour, A., Leboeuf, C., Flahaut, S., Auffray, Y., and Hartke, A. (2001) The stress proteome of *Enterococcus faecalis*. *Electrophoresis.* **22,** 2947–2954
24. Wang, X., He, X., Jiang, Z., Wang, J., Chen, X., Liu, D., Wang, F., Guo, Y., Zhao, J., Liu, F., Huang, L., and Yuan, J. (2010) Proteomic analysis of the *Enterococcus faecalis* V583 strain and clinical isolate V309 under vancomycin treatment. *J. Proteome Res*. **9,** 1772–1785
25. Pessione, A., Lamberti, C., Cocolin, L., Campolongo, S., Grunau, A., Giubergia, S., Eberl, L., Riedel, K., and Pessione, E. (2012) Different protein expression profiles in cheese and clinical isolates of *Enterococcus faecalis* revealed by proteomic analysis. *Proteomics.* **12,** 431–447
26. Bøhle, L. A., Færgestad, E. M., Veiseth-Kent, E., Steinmoen, H., Nes, I. F., Eijsink, V. G., and Mathiesen, G. (2010) Identification of proteins related to the stress response in *Enterococcus faecalis* V583 caused by bovine bile. *Proteome Sci.* **8,** 37
27. Seneviratne, C. J., Suriyanarayanan, T., Swarup, S., Chia, K. H. B., Nagarajan, N., and Zhang, C. (2017) Transcriptomics analysis reveals putative genes involved in biofilm formation and biofilm-associated drug resistance of *Enterococcus faecalis*. *J. Endod.* **43,** 949–955
28. Seneviratne, C. J., Yip, J. W., Chang, J. W., Zhang, C. F., and Samaranayake, L. P. (2013) Effect of culture media and nutrients on biofilm growth kinetics of laboratory and clinical strains of *Enterococcus faecalis*. *Arch. Oral Biol.* **58,** 1327–1334
29. Ghosh, D., Li, Z., Tan, X. F., Lim, T. K., Mao, Y., and Lin, Q. (2013) iTRAQ based quantitative proteomics approach validated the role of calcyclin binding protein (CacyBP) in promoting colorectal cancer metastasis. *Mol. Cell. Proteomics* **12,** 1865–1880
30. Gao, Y., Lim, T. K., Lin, Q., and Li, S. F. Y. (2016) Identification of cypermethrin induced protein changes in green algae by iTRAQ quantitative proteomics. *J. Proteomics* **139,** 67–76

31. Strbenac, D., Zhong, L., Raftery, M. J., Wang, P., Wilson, S. R., Armstrong, N. J., Wang, P., Wilson, S. R., Armstrong, N. J., and Yang, J. Y. H. (2017) Quantitative performance evaluator for proteomics (QPEP): Web-based application for reproducible evaluation of proteomics preprocessing methods. *J. Proteome Res.* **16,** 2359–2369
32. Ghosh, D., Yu, H., Tan, X. F., Lim, T. K., Zubaidah, R. M., Tan, H. T., Chung, M. C., and Lin, Q. (2011) Identification of key players for colorectal cancer metastasis by iTRAQ quantitative proteomics profiling of isogenic SW480 and SW620 cell lines. *J. Proteome Res.* **10,** 4373–4387
33. Gan, C. S., Chong, P. K., Pham, T. K., and Wright, P. C. (2007) Technical, experimental, and biological variations in isobaric tags for relative and absolute quantitation (iTRAQ). *J. Proteome Res.* **6,** 821–827
34. Christmas, R., Avila-Campillo, I., Bolouri, H., Schwikowski, B., Anderson, M., Kelley, R., Landys, N., Workman, C., Ideker, T., Cerami, E., Sheridan, R., Bader, G. D., and Sander C. (2005) Cytoscape: A software environment for integrated models of biomolecular interaction networks. *AACR Educ. Book* **2005,** 12–16
35. Maere, S., Heymans, K., and Kuiper, M. (2005) BiNGO: A Cytoscape plugin to assess overrepresentation of bene ontology categories in biological networks. *Bioinformatics* **21,** 3448–3449
36. Li, P., Seneviratne, C. J., Alpi, E., Vizcaino, J. A., and Jin, L. (2015) Delicate metabolic control and coordinated stress response critically determine antifungal tolerance of *Candida albicans* biofilm persisters. *Antimicrob. Agents Chemother.* **59,** 6101–6112
37. Griffin, H. G., and Gasson, M. J. (1995) The gene (*aroK*) encoding shikimate kinase I from *Escherichia coli*. *DNA Seq.* **5,** 195–197
38. Priestman, M. A., Funke, T., Singh, I. M., Crupper, S. S., and Schönbrunn, E. (2005) 5-enolpyruvylshikimate-3-phosphate synthase from *Staphylococcus aureus* is insensitive to glyphosate. *FEBS Lett.* **579,** 728–732
39. Andersson, U., Levander, F., and Rådström, P. (2001) Trehalose-6-phosphate phosphorylase is part of a novel metabolic pathway for trehalose utilization in *Lactococcus lactis*. *J. Biol. Chem.* **276,** 42707–42713
40. Karinou, E., Compton, E. L., Morel, M., and Javelle, A. (2013) The *Escherichia coli* SLC26 homologue YchM (DauA) is a C4-dicarboxylic acid transporter. *Mol. Microbiol.* **87,** 623–640
41. Zolotarev, A. S., Unnikrishnan, M., Shmukler, B. E., Clark, J. S., Vandorpe, H., Grigorieff, N., Rubin, E. J., and Alper, S. L. (2009) Increased sulfate uptake by *E. coli* overexpressing the SLC26-related SulP protein Rv1739c from *Mycobacterium tuberculosis*. *Comp. Biochem. Physiol.* **149,** 255–266
42. Janosi, L., Shimizu, I., and Kaji, A. (1994) Ribosome recycling factor (ribosome releasing factor) is essential for bacterial growth. *Proc. Natl. Acad. Sci. U.S.A.* **91,** 4249–4253
43. Almiron, M., Link, A. J., Furlong, D., and Kolter, R. (1992) A novel DNA-binding protein with regulatory and protective roles in starved *Escherichia coli*. *Genes Dev.* **6,** 2646–2654,
44. Vaillancourt, K., Moineau, S., Frenette, M., Lessard, C., and Vadeboncoeur, C. (2002) Galactose and lactose genes from the galactose-positive bacterium *Streptococcus salivarius* and the phylogenetically related galactose-negative bacterium *Streptococcus thermophilus*: Organization, sequence, transcription, and activity of the gal gene produc. *J. Bacteriol.* **184,** 785–793
45. Mikalsen, T., Pedersen, T., Willems, R., Coque, T. M., Werner, G., Sadowy, E., van Schaik, W., Jensen, L. B., Sundsfjord, A., and Hegstad, K. (2015) Investigating the mobilome in clinically important lineages of *Enterococcus faecium* and *Enterococcus faecalis*. *BMC Genomics.* **16,** 282
46. Hegstad, K., Mikalsen, T., Coque, T. M., Werner, G., and Sundsfjord, A. (2010) Mobile genetic elements and their contribution to the emergence of antimicrobial resistant *Enterococcus faecalis* and *Enterococcus faecium*. *Clin. Microbiol. Infect*. **16,** 541–554.
47. Bryers, J. D. (2009) Medical biofilms. *Biotechnol. Bioeng.* **100,** 1–18.
48. Alexander, J. W. (1973) Nosocomial infections. *Curr. Probl. Surg.* **10,** 1–54
49. Karki, H. S., and Ham, J. H. (2014) The roles of the shikimate pathway genes, aroA and aroB, in virulence, growth and UV tolerance of *Burkholderia glumae* strain 411gr-6. *Mol. Plant Pathol.* **15,** 940–947
50. Orihuela, C. J., Gao, G., Francis, K. P., Yu, J., and Tuomanen, E. I. (2004) Tissue-specific contributions of pneumococcal virulence factors to pathogenesis. *J. Infect. Dis.* **190,** 1661–1669
51. Ogunniyi, A. D., Mahdi, L. K., Trappetti, C., Verhoeven, N., Mermans, D., Van der Hoek, M. B., Plumptre, C. D., and Paton, J. C. (2012) Identification of genes that contribute to the pathogenesis of invasive pneumococcal disease by in vivo transcriptomic analysis. *Infect. Immun.* **80,** 3268–3278
52. Iyer, R., and Camilli, A. (2007) Sucrose metabolism contributes to in vivo fitness of *Streptococcus pneumoniae*. *Mol. Microbiol.* **66,** 1–13
53. Mah, T. F., and O'Toole, G. A. (2001) Mechanisms of biofilm resistance to antimicrobial agents. *Trends Microbiol.* **9,** 34–39
54. Van Acker, H., Sass, A., Bazzini, S., De Roy, K., Udine, C., Messiaen, T., Riccardi, G., Boon, N., Nelis, H. J., Mahenthiralingam, E., and Coenye, T. (2013) Biofilm-grown *Burkholderia cepacia* complex cells survive antibiotic treatment by avoiding production of reactive oxygen species. *PLoS ONE* **8,** e58943
55. Zhang, L., Chiang, W. C., Gao, Q., Givskov, M., Tolker-Nielsen, T., Yang, L., and Zhang, G. (2012) The catabolite repression control protein *Crc* plays a role in the development of antimicrobial-tolerant subpopulations in *Pseudomonas aeruginosa* biofilms. *Microbiology* **158,** 3014–3019
56. Klein, M. I., Xiao, J., Lu, B., Delahunty, C. M., Yates, J. R., 3rd, and Koo, H. (2012) *Streptococcus mutans* protein synthesis during mixed-species biofilm development by high-throughput quantitative proteomics. *PLoS ONE* **7,** e45795
57. Bao, K., Bostanci, N., Thurnheer, T., and Belibasakis, G. N. (2017) Proteomic shifts in multi-species oral biofilms caused by *Anaeroglobus geminatus*. *Sci. Rep.* **7,** 4409